



Rapid, high sensitivity, point-of-care test for cardiac troponin based on optomagnetic biosensor

Wendy U. Dittmer^{a,*}, Toon H. Evers^a, Willie M. Hardeman^a, Willeke Huijnen^a, Rick Kamps^a, Peggy de Kievit^a, Jaap H.M. Neijzen^a, Jeroen H. Nieuwenhuis^a, Mara J.J. Sijbers^a, Dave W.C. Dekkers^b, Marco H. Hefti^b, Mike F.W.C. Martens^b

^a Philips Corporate Technologies, Eindhoven, The Netherlands

^b Future Diagnostics BV, Wijchen, The Netherlands

ARTICLE INFO

Article history:

Received 8 December 2009

Received in revised form 1 March 2010

Accepted 1 March 2010

Available online 6 March 2010

Keywords:

Magnetic particles

Electromagnet

Finger-prick blood

Dry reagents

Dynamic range

Evanescence fields

ABSTRACT

Background: We present a prototype handheld device based on a newly developed optomagnetic technology for the sensitive detection of cardiac troponin I (cTnI) in a finger-prick blood sample with a turnaround time of 5 min.

Methods: The test was completed in a compact plastic disposable with on-board dry reagents and superparamagnetic nanoparticles. In our one-step assay, all reaction processes were precisely controlled using electromagnets positioned above and below the disposable. Nanoparticle labels (500 nm) bound to the sensor surface via a sandwich immunoassay were detected using the optical technique of frustrated total internal reflection.

Results: A calibration function measured in plasma demonstrates a limit of detection (mean of blank plus 3-fold the standard deviation) of 0.03 ng/mL cTnI. A linear regression analysis of the region 0.03–6.5 ng/mL yields a slope of 37 ± 4 , and a linear correlation coefficient of $R^2 = 0.98$. The measuring range could be extended substantially to 100 ng/mL by simultaneously imaging a second spot with a lower antibody concentration.

Conclusions: The combination of magnetic particles and their fine actuation with electromagnets permits the rapid and sensitive detection of cTnI. Because of the potential high analytical performance and ease-of-use of the test, it is well suited for demanding point-of-care diagnostic applications.

© 2010 Elsevier B.V. All rights reserved.

1. Introduction

The development of technologies that deliver high performance in a format suitable for the point-of-care is a difficult challenge. Not only must the analytical requirements such as high sensitivity and precision be fulfilled but the test must be fast, integrated for ease-of-use, robust, and low cost and preferably be in a portable or handheld form [1,2]. Magnetic nanoparticles are often used to increase the speed and sensitivity of analytical quantifications by being a carrier for reagent or analyte concentration [3,4]. They can also be employed as particulate labels in immunoassays and nucleic acid testing [5–8]. The ability to finely manipulate magnetic nanoparticles with a magnetic field [5,6,9,10] makes them suitable for enhancing the speed and for the integration of various assay processes in a high performance test for the point-of-care. We have recently reported an

optomagnetic technology that combines the precise control of the motion of magnetic particles with electromagnets and their sensitive detection on a surface using f-TIR imaging [11]. The optomagnetic biosensor platform offers speed, sensitivity and a high degree of analyte multiplexing. The technology can potentially be used in conjunction with any label-based affinity assay for the detection of a wide range of analytes including proteins, small molecules and nucleic acids. Its compact, robust form along with the use of a low cost, mass-manufacturable plastic disposable is very advantageous for the POC environment.

An example of a high performance assay that is desirable to have in a POC format, is the testing for cardiac markers in the diagnosis of acute coronary syndrome due to the time critical nature of the disease [12]. Cardiac troponin I and T (cTnI, cTnT) are markers highly specific for myocardial damage. They can be used alone or in combination with other cardiac markers (e.g. CK-MB, myoglobin) to positively diagnose an acute myocardial infarction [13]. As the recommended clinical cutoff for troponin is the 99th percentile (0.01 ng/mL concentration range) [14], assays for this marker must be highly sensitive and precise. There is a variety of detection technologies utilized in POC devices, including immunochromatographic assays (employing for example, Au nanoparticles or fluorescent molecules/

Abbreviations: f-TIR, frustrated total internal reflection; POC, point-of-care; cTnI, cTnT, cardiac troponin I and T; MES, 2-(N-morpholino)ethanesulfonic acid; EDC, N-3-dimethylaminopropyl-N-ethylcarbodiimide hydrochloride.

* Corresponding author. Philips Corporate Technologies, High Tech Campus 11, 5656 AE Eindhoven, The Netherlands. Tel.: +31 40 2741774; fax: +31 40 2742944.

E-mail address: wendy.dittmer@philips.com (W.U. Dittmer).

particles as labels) [15–17], and enzyme-linked immunosorbent assays (with electrochemical or optical detection) [18]. However, very few can offer sensitive and precise troponin testing in a handheld or portable format. The majority of POC tests for cardiac markers are desktop devices that require either long turnaround times (>10 min), large sample volumes (>100 μL) or sample pre-treatment, all of which significantly decrease the ease-of-use of the device [19]. Of the existing POC handheld technologies, even fewer are able to rapidly deliver a sensitive and precise troponin result from a finger-prick blood volume [20,21].

We have developed a sensitive, 5-minute prototype POC test for cTnI using the optomagnetic biosensor. The test is a one-step sandwich immunoassay performed in a stationary liquid in which all assay processes are integrated by the use of magnetic forces acting on magnetic nanoparticle labels (Fig. 1). In the first phase of the assay, nanoparticles highly loaded with antibody move through the solution for effective troponin molecule capture. Subsequently actuating magnets are engaged to move and transport the particles with high speed to the sensor surface for binding. Thereafter, a sequence of finely tuned magnetic pulses is applied to facilitate optimal binding and mixing of the nanoparticles containing cTnI molecules at the antibody-functionalized surface. After the particles react with the sensor surface, free and non-specifically bound particles are rapidly removed with a magnetic wash by applying a magnetic field oriented away from the detection surface. Seamless integration of the assay steps facilitate the design of a simple, single-chamber cartridge, in which dry reagents, including magnetic particles are deposited. The absence of a fluidic wash or fluidic handling enables the use of very small assay volumes, on the order of 1 μL , which easily accommodates finger-prick blood samples. The results described provide a proof-of-principle of the analytical performance achievable using the optomagnetic technology and offer a basis for further optimizations necessary to achieve the same challenging precision requirements demanded of laboratory cTnI tests.

2. Materials and methods

2.1. Reagents

All buffer materials unless otherwise stated were supplied by Sigma Aldrich Corporation. Superparamagnetic particles functionalized with carboxylic acid groups (MasterBeads 500 nm diameter) were purchased from Ademtech. A number of antibody pairs recognizing various epitopes on cTnI were screened and found to be very effective for the detection of cTnI using the optomagnetic biosensor technology. In this work we focus on results from the pair consisting of the monoclonal antibody A34780359P (BiosPacific Inc.) as the tracer coupled to the particles, and goat polyclonal (Hytest Ltd)

as the capture antibody immobilized on the sensor surface. Calibrators were prepared from human troponin ITC complex (Hytest, reference SRM(r)2921) by diluting either in pure human citrate plasma pool from 20 apparently healthy donors or in EDTA whole blood from single healthy donors. Concentration values stated in this work were based on serial dilutions made directly in citrate plasma or EDTA whole blood. In experiments with whole blood, the samples were used within 12 h of collection to avoid effects from degradation.

2.2. Optomagnetic biosensor platform

Fig. 2A shows a schematic of the optomagnetic analyzer/reader consisting of the f-TIR detection optics and the actuating electromagnetic coils [11]. These were designed for and incorporated into a handheld format, a fully functional experimental version of which is displayed in Fig. 2B. For the data presented in this report, an open laboratory setup, interfaced with a personal computer, was used in order to collect more detailed data and to have more setup modification flexibility.

The analyzer was used in combination with an injection-molded disposable cartridge containing a reaction chamber for the assay (Fig. 2C). The bottom surface of the reaction chamber was functionalized with capture antibody and served as the sensing surface. Magnetic nanoparticles at the sensor surface were detected using the optical principle of frustrated total internal reflection (f-TIR) [11,22,23]. Systems for f-TIR imaging are well suited for near-patient applications because they take advantage of the superior performance of optical detection (high sensitivity, multiplexing, insensitivity to magnetic fields and chemical interference) while being robust, low cost and readily integrated into a portable format. The signal at time t was calculated for each spot, averaging over an area of approximately $100 \times 100 \mu\text{m}$, using the formula $\text{Signal}(t) = [R(0) - R(t)]/R(0)$, where $R(0)$ is the reflected light intensity in the absence of magnetic particles at the sensor surface and $R(t)$ is the reflected light intensity at time t during the assay. The end point signal for an assay was determined from the difference between the signal upon sample introduction into the chamber and signal after the magnetic wash (see section III of Fig. 3A). The current optics in our f-TIR setup enables microarrays consisting of more than 30 distinct spots ($\sim 100 \mu\text{m}$ diameter) to be simultaneously imaged. In Fig. 2D, the f-TIR image of an array consisting of four spots is shown. By printing different capture antibodies on the spots and using a mixture of magnetic particles with the corresponding tracer antibodies, it is possible to multiplex a high number of different analytes.

The actuating electromagnets consist of two magnetic systems, a top coil 2 mm above the sensor surface and a bottom magnet system positioned 1 mm below the sensing surface. The magnetic flux was

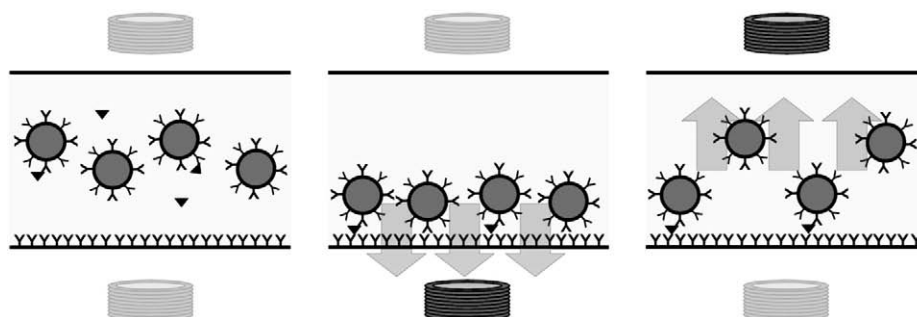


Fig. 1. Depiction of the reaction chamber and actuation magnets showing successively the assay processes: analyte binding by antibody-functionalized nanoparticles (top and bottom magnets off), nanoparticle binding to the sensor surface and magnetic removal of free and weakly bound nanoparticles.

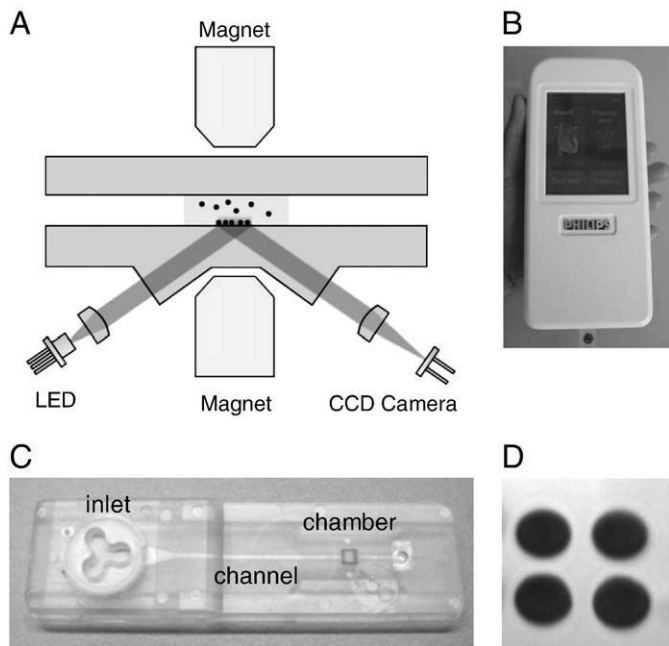


Fig. 2. A) Schematic of the optomagnetic analyzer/reader consisting of the top and bottom magnets and the detection optics. The presence of nanoparticles attached to the sensor surface is determined by illuminating the cartridge above the critical angle and measuring the decrease in reflected light. B) Picture of a functional handheld reader comprising f-TIR optics and actuation magnets. C) Picture of an assembled disposable cartridge comprising two structured plastic parts connected by doubled-sided tape. The structures define a sample inlet containing the plasma filter, channel, 0.4 μL reaction chamber with dry magnetic particles and vent. D) f-TIR image of four spots of 200 μm diameter with magnetic nanoparticles bound to the sensor surface via an immunoassay.

generated by copper coils which were wound around a 2.5 mm cobalt–iron alloy core. Each of the magnets in the system can be independently electronically controlled.

2.3. Fabrication of disposable cartridge

Magnetic nanoparticles were functionalized with tracer antibody according to the one-step coating procedure described by Dynal Biotech (Life Technologies). For deposition and drying of the particles in the cartridge chamber, they were resuspended in a drying buffer (50 g/L sucrose, 50 g/L BSA in PBS) at a concentration of 10 g/L. Three hundred nanoliters of the solution was deposited into a cavity in the top plastic part of the cartridge and dried under a desiccated atmosphere provided by silica at 4 $^{\circ}\text{C}$ for at least 12 h. The plastic top part of the cartridge was injection molded from polystyrene in-house.

The plastic bottom part of the disposable comprising the sensor surface was formed by the injection molding of high binding microtiter plate substrate material. Spots of 200 μm diameter were inkjet printed with a sciFLEXARRAYER S5 (Scienion AG) using a 2 nL print volume of capture antibody solution (150 mg/L in PBS). The printed substrates were dried for 3 min at 37 $^{\circ}\text{C}$ and then washed three times with 500 μL washing buffer (0.5 g/L Tween-20 in PBS) to remove excess protein. Thereafter the sensor surface was further blocked (10 g/L BSA and 100 g/L sucrose in PBS) for at least 1 h. Finally, excess buffer was drained and the substrates were dry sealed with silica pouches for at least 12 h at 4 $^{\circ}\text{C}$.

The disposable was assembled by connecting the structured top and bottom plastic parts with 180 μm thick double-sided, biocompatible adhesive tape which was laser cut to form a sample inlet, microfluidic channel, either a 0.5 or 0.8 μL reaction chamber and a vent (Fig. 2C). In assays performed with whole blood, a blood separation filter (Pall Corp.) was added at the sample inlet and a

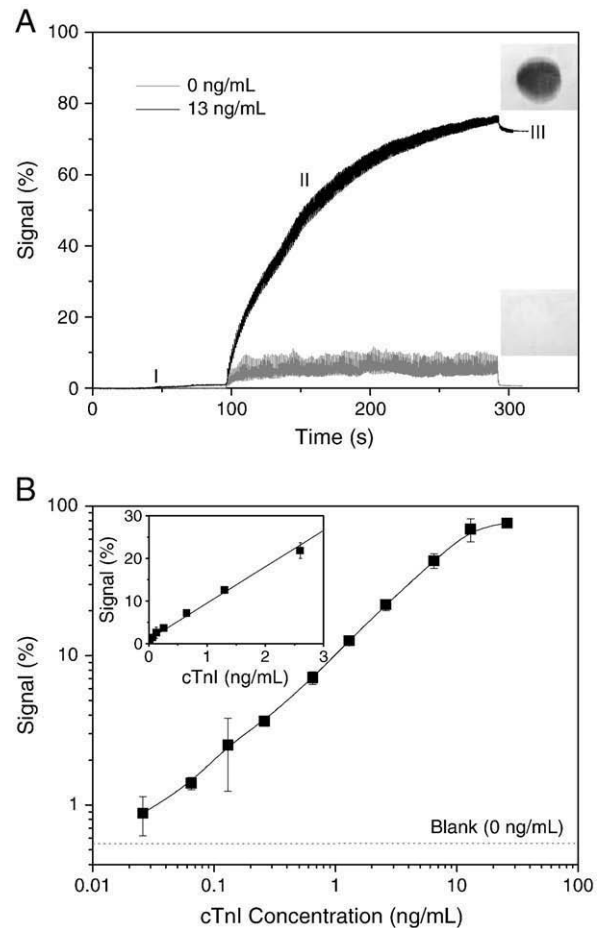


Fig. 3. A) Real-time trace of the optical f-TIR signal during a sandwich assay for cTnI concentrations of 0 and 13 ng/mL in 100% plasma. In section I dry nanoparticles redisperse and bind cTnI molecules in the sample. In section II particles bind at the sensor surface using a pulsed actuation protocol. In section III weakly and unbound particles are removed with a magnetic force directed away from the surface using the top coil. The corresponding f-TIR images are shown of the spots after the magnetic wash. B) A calibration curve of the final optical f-TIR signal after the magnetic removal step as a function of cTnI concentration for a 5-minute assay in 100% plasma, in a reaction chamber volume of 0.8 μL . The line connecting the points serves as a guide to the eye only. The inset shows a linear fit of the calibration curve for range 0.03–6.5 ng/mL cTnI.

100 μm connecting tape was used to enable rapid capillary filling of the chamber with the generated plasma.

2.4. Performing the assay

The cTnI tests were performed by injecting either 10 μL of spiked plasma pool sample or 25 μL of spiked whole blood into the inlet of the cartridge. After complete filling of the reaction chamber, the actuation protocol was initiated. In the first 90 s of the assay during which the magnets were off, particles and buffer components redisperse from the dry form and bind with the cTnI analyte in the sample fluid. Thereafter a magnetic field with alternating orientation is applied for 195 s (field strength $3 \cdot 10^4$ A/m). The particle binding and mixing actuation scheme alternately attracts the particles toward and away from the sensor surface [11]. In a final step, the magnetic wash, the bottom magnet was turned off and the top electromagnetic coil was powered (field strength $2 \cdot 10^4$ A/m) to pull the unbound particles away from the sensor surface for 10 s. The total assay time was 5 min. Unless otherwise stated all data points are from assays performed in triplicate.

3. Results and discussion

In our one-step cTnI assay, all the assay processes have been magnetically integrated to transpire in a single microchamber. Fig. 3A displays the f-TIR signal, measured in real-time, in the chamber of a magnetic-label sandwich assay for 0 and 13 ng/mL cTnI in undiluted plasma. In the first 90 s, while dried-in particles are redispersed by the addition of sample and bind cTnI molecules present in the solution with magnetic fields off, the signal does not change significantly. Only a few particles that diffuse and sediment from the top part of the chamber reach the sensor surface (section I of Fig. 3A). As soon as the magnets are engaged particles are rapidly attracted towards and collected at the surface. Subsequently, a pulsating magnetic actuation sequence is applied for 4 min to bind particles containing cTnI to the sensor surface, resulting in a steep rise in the signal (section II of Fig. 3A). The rate of signal increase is greater for higher cTnI concentrations since the fraction of bound particles will be larger and, on average, contribute more to the signal as they are closer to the surface than particles freely diffusing in (and out of) the evanescent field. The amount of particles specifically bound to the sensor surface is measured after the application of a magnetic separation step, continuing for 10 s, to remove free and weakly bound particles (section III of Fig. 3A). The entire assay (sample in, result out) is completed in approximately 5 min. The corresponding f-TIR image of the sensor surface from the 13 ng/mL cTnI assay displays the dark spot containing bound magnetic particles with a relatively low background observed outside the spot (signal-to-background ratio > 70). However, we observe that the non-specific binding of particles within the spot containing capture antibodies is approximately 2-fold lower than in the surrounding regions which are blocked with BSA. In the f-TIR image of the blank no significant signal from non-specifically bound particles inside the spot is discernible above the background noise of the system. Therefore, the corresponding signal-to-blank ratio exceeds 100 at 13 ng/mL cTnI.

A calibration function (Fig. 3B) of the sensor signal after the magnetic wash yields a limit of detection of 0.03 ng/mL (1 pM) cTnI in 100% plasma (based on 3-fold the standard deviation of the blank). A linear regression analysis of the region 0.03–6.5 ng/mL yields a slope of 37 ± 4 , an intercept of 0.22 ± 0.01 and a linear correlation coefficient of $R^2 = 0.98$ (Fig. 3B, inset). In contrast to reports by others of highly sublinear behavior of immunoassays using magnetic particles as labels [7,8], our calibration curve is linear which we attribute to the magnetic actuation procedure and the linear dependence of the f-TIR signal on the particle surface density. The intra-assay imprecision in signal of ten cTnI standards at 0.5 ng/mL in plasma is 14%. As the disposables in the current report are manually processed and assembled, substantial improvements are expected when the fabrication process is automated. The fine magnetic control of the assay reduces variation which may arise from, among others, incubation times, and the free/bound separation of tracer antibody. The magnetic actuation therefore, intrinsically permits the creation of highly precise tests.

Immunoassays based on particle labels often have a lower measuring range than those based on molecular labels due to the sizeable space occupied by a single particle on the capture surface. In our assay at concentrations greater than 13 ng/mL cTnI, the signal saturates as the spot surface reaches full particle coverage (Fig. 3B). The imaging properties of f-TIR technology are not only highly advantageous for multiplex detection of several analytes but also offer a simple method to extend the dynamic range of the cTnI assay. Fig. 4 displays f-TIR images of endpoint measurements for cTnI at 13, 65 and 98 ng/mL in which two spots were printed, one with the standard 150 $\mu\text{g/mL}$ and the second at a significantly lower 9.4 $\mu\text{g/mL}$ polyclonal antibody concentration. The lower concentration spot was supplemented with non-specific goat IgG to a total protein concentration of 150 $\mu\text{g/mL}$. The presence of non-specific IgG maintains the

printing, drying and washing characteristics of the spotting process and is intended to preserve the resulting capture antibody activity on the sensor surface. From the image of the 150 $\mu\text{g/mL}$ antibody spot, full surface coverage of particles is observed at 13 ng/mL cTnI and above. However, on the same f-TIR images, the 9.4 $\mu\text{g/mL}$ antibody spot shows a substantial difference in number of bound particles between 13, 65 and 98 ng/mL cTnI. A calibration curve based on the 9.4 $\mu\text{g/mL}$ antibody spot indicates that concentrations up to 100 ng/mL cTnI can be measured. For high sensitivity, low concentration quantifications, the 150 $\mu\text{g/mL}$ antibody spot can be employed and at analyte concentrations above saturation, the 9.4 $\mu\text{g/mL}$ antibody spot can be used. By performing one single assay on an array consisting of two spots and using an algorithm that combines the respective calibration curves, the measuring range for cTnI can be increased by approximately 10-fold. For analytes that require dynamic ranges substantially larger than 1000, more than two spots can be implemented, given that the antibody in the spot can be sufficiently diluted and still maintain its activity. Quantification of high concentrations of analyte using the one-step sandwich immunoassay format is often limited by the high-dose hook effect, in which both the capture and tracer antibodies are independently occupied with analyte. This effect can result in a false negative clinical result for patients with high analyte levels. Based on the calibration curve using the 150 $\mu\text{g/mL}$ antibody spot in Fig. 4, our cTnI magnetic-label assay does not show a high-dose hook effect up to concentrations of 130 ng/mL cTnI. This is likely a consequence of the large surface area of the particles ($3 \cdot 10^{-9} \text{ m}^2$), on which tracer antibody is coupled, compared to the capture antibody-functionalized sensor spot area ($3 \cdot 10^{-8} \text{ m}^2$). At the relatively high tracer concentrations, the kinetics is more favorable for analyte binding to the tracer than to the capture antibody (given that the kinetic association constants for both tracer and capture antibodies are similar). The binding capacity for cTnI of the tracer antibodies on the nanoparticles is so high that we have not observed a high-dose hook effect even up to 6.5 $\mu\text{g/mL}$ cTnI (data not shown).

The magnetic integration of assay processes eases fluidic and functional integration requirements in the disposable. In our assay the incubation time of the various assay processes can be precisely controlled by the electromagnets unlike other POC technologies which often control

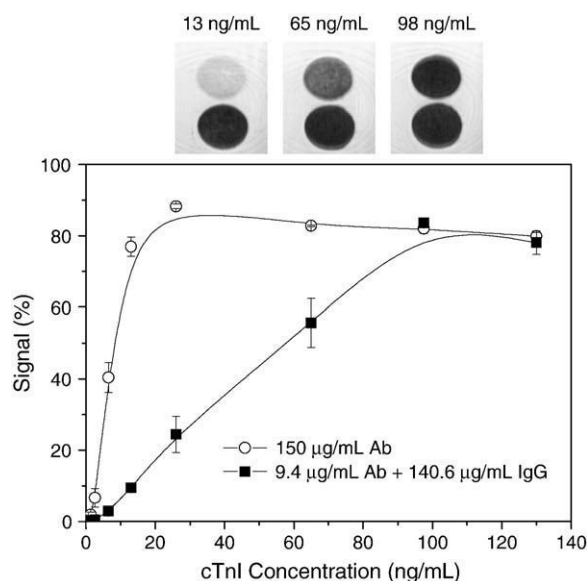


Fig. 4. f-TIR images of cTnI assay for various analyte concentrations in 100% plasma after the magnetic wash showing two printed capture spots. The top spot was printed from a solution of 9.4 $\mu\text{g/mL}$ polyclonal antibody and 140.6 $\mu\text{g/mL}$ goat IgG and the bottom spot was printed from a solution containing 150 $\mu\text{g/mL}$ polyclonal antibody. A calibration curve of the f-TIR signal after the magnetic wash as a function of cTnI concentration for the top and bottom spots is displayed. The line connecting the points serves as a guide only. The reaction chamber volume is 0.5 μL .

incubation time using functional characteristics in the disposable [24]. For example, the incubation time is dependent on the flow properties in immunochromatographic assays, which can be controlled by the substrate material properties (e.g. immunochromatographic strips) [17], or by microfluidic structures on the surface of the disposable [15]. Performing assays in a stationary fluid has the advantage that reagents (particles and buffers) can be directly deposited in the reaction chamber where they can be monitored during the entire assay. Moreover, in the absence of flow, it is not necessary to tune the release profile of the reagents into the solution. We have developed buffers and conditions for depositing and storing dry magnetic particles for full reagent integration in the disposal. The dried-in magnetic particles release completely within several seconds after application of the sample. Addition of a sugar and blocking protein to the buffer for drying prevents the particles from adhering to the plastic cavity in which they are deposited, and allow the homogeneous redispersion of monodisperse particles, without significantly disturbing the function of the antibodies in the assay. In order for the disposables with the dry reagents to have a long shelf-life, it is necessary to avoid the formation of permanent particle clusters, which can be a consequence of the long particle–particle interaction time in the immobilized state. Dry reagent instability can result in slow redispersion or redispersion of particles as aggregates upon sample addition, both of which are detrimental to the assay. Fig. 5A displays the signal at 0 and

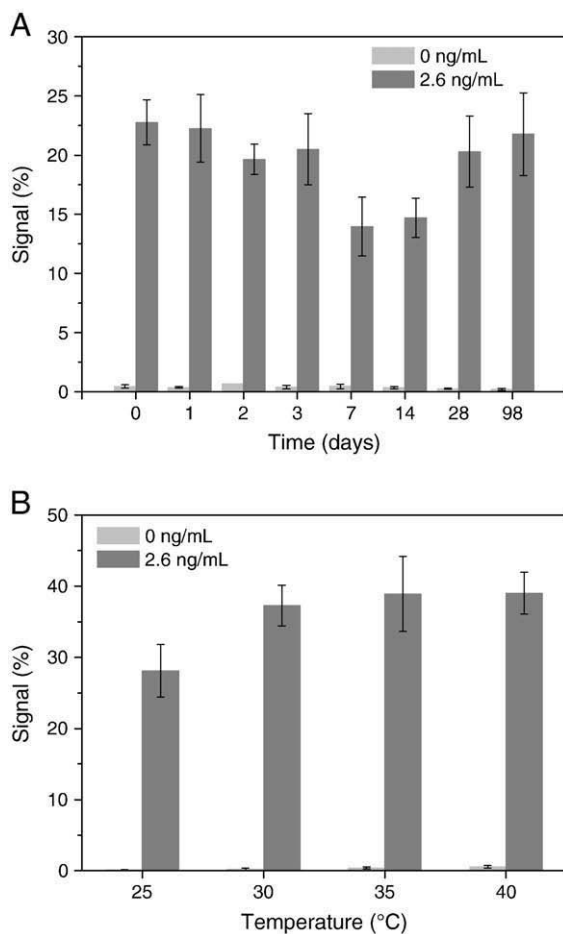


Fig. 5. A) Real-time aging studies for disposables printed with goat polyclonal on the sensor surface and dried-in magnetic particles and buffer components. The cartridges were stored with silica at 4 °C. End point f-TIR measurements are shown ($n=10$). B) Temperature dependence of cTnI assay performance in 100% plasma, in a reaction chamber volume of 0.5 μ L. End point f-TIR measurements are shown ($n=6$). The analyzer, sample and cartridges were all equilibrated to the desired temperature in a sealed climate chamber (Espec PL-2KPH) at ambient humidity. cTnI samples were exposed to elevated temperatures for less than 10 min to avoid degradation.

2.6 ng/mL cTnI, for cartridges containing the described dry components stored at 4 °C over 14 weeks. The dry reagents integrated into the disposable are stable and there is no substantial change in assay performance over this period. The dry reagent composition is robust and assays completed at elevated temperatures with these reagents show no indications of irreversible cluster development. In Fig. 5B, it can be seen that the assay in 100% plasma is functional up to at least 40 °C. At higher temperatures the blank signal increases slightly due to greater non-specific interactions. The optimal operating temperature lies in a broad range between 25 and 40 °C.

The small volume required in our single-chamber magnetic particle immunoassay and the integration of dry reagents in the disposable facilitates the direct use of finger-prick blood samples. To generate plasma from whole blood, a blood separation filter was incorporated into the sample inlet of the disposable. From 25 μ L of blood, typical of a finger-prick, only 1 μ L of plasma is required for the assay. Due to the low fill volume of the disposable, the blood separation and capillary filling can occur in less than 30 s which when coupled with an assay requiring 5 min, results in a very fast turnaround time. Fig. 6 displays the performance of an approximately 5 min cTnI assay in a fully integrated disposable for 25 μ L of spiked whole blood sample. The filter used in this experiment apparently exhibits some affinity for cTnI molecules and thus lowers the recovery values. We are investigating a number of filter blocking procedures in order to reduce this effect.

For a cTnI POC test to be accepted in a clinical practice, high precision quantification at low analyte concentrations is necessary. Unfortunately very few commercial POC tests have been able to demonstrate the recommended criterion for cTnI (10% CV at the clinical cutoff [14]). We provide one potential technology solution that can carry out high performance analyses in an integrated, convenient format. In the next stages of our work, it will be necessary to validate the test with patient samples in a clinical setting to determine whether the highly demanding precision criteria for cTnI can be achieved under the strict ease-of-use constraints typical of near-patient settings. In addition, disposables with built-in fail-safes and calibrators for reagent variability are necessary to ensure high test result reproducibility under a wide variety of manufacturing and user conditions. The testing of cardiac markers in acute settings is one application of the new technology platform. The short assay time and microliter assay volume required by the device open up a broad range of other opportunities for sensitive and precise testing in demanding point-of-care environments, including the ambulance, hospital, physician's office and the home of patients.

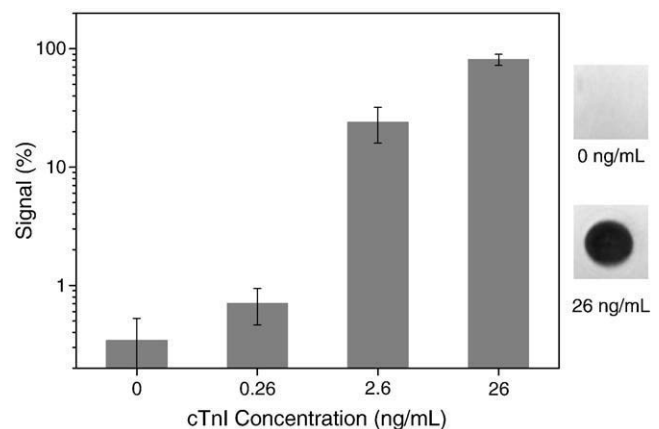


Fig. 6. Endpoint f-TIR signal for 5-minute assays using a sample of 25 μ L of cTnI spiked whole blood at several concentrations. The f-TIR images of the sensor surface after the magnetic wash of assays performed with 0 and 26 ng/mL cTnI are inserted. The assays were performed in disposables containing a blood separation filter and on-cartridge dry reagents in a reaction chamber with a volume of 0.4 μ L (See Fig. 2C).

Conflict of interest

All authors are employed either by Philips Electronics Netherland or Future Diagnostics.

Acknowledgements

The authors would like to thank M. Prins for helpful discussions. D. Bruls is gratefully acknowledged for providing technical assistance. The work was partially funded by the Dutch Ministry of Economic Affairs under the NanoNed program (Nanofluidics) and the European Union under the FP6 program (project DiaNa).

References

- [1] Warsinke A. Point-of-care testing of proteins. *Anal Bioanal Chem* 2009;393:1393–405.
- [2] von Lode P. Point-of-care immunotesting: approaching the analytical performance of central laboratory methods. *Clin Biochem* 2005;38:591–606.
- [3] Todd J, Freese B, Lu A, et al. Ultrasensitive flow-based immunoassays using single-molecule counting. *Clin Chem* 2007;53:1990–5.
- [4] Do J, Ahn CH. A polymer lab-on-a-chip for magnetic immunoassay with on-chip sampling and detection capabilities. *Lab Chip* 2008;8:542–9.
- [5] Koets M, van der Wijk T, van Eemeren JTWM, van Amerongen A, Prins MWJ. Rapid DNA multi-analyte immunoassay on a magneto-resistance biosensor. *Biosens Bioelectron* 2009;24:1893–8.
- [6] Dittmer WU, de Kievit P, Prins MWJ, Vissers JLM, Mersch MEC, Martens MFWC. Sensitive and rapid immunoassay for parathyroid hormone using magnetic particle labels and magnetic actuation. *J Immunol Methods* 2008;338:40–6.
- [7] Mulvaney SP, Myers KM, Sheehan PE, Whitman LJ. Attomolar protein detection in complex sample matrices with semi-homogeneous fluidic force discrimination assays. *Biosens Bioelectron* 2009;24:1109–15.
- [8] Osterfeld SJ, Yu H, Gaster RS, et al. Multiplex protein assays based on real-time magnetic nanotag sensing. *Proc Natl Acad Sci U S A* 2008;105:20637–40.
- [9] Morozov VN, Morozova TY. Active bead-linked immunoassay on protein microarrays. *Anal Chim Acta* 2006;564:40–52.
- [10] Janssen XJA, van IJzendoorn IJ, Prins MW. On-chip manipulation and detection of magnetic particles for functional biosensors. *Biosens Bioelectron* 2008;23:833–83.
- [11] Bruls DM, Evers TH, Kahlman JAH, et al. Rapid integrated biosensor for multiplexed immunoassays based on actuated magnetic nanoparticles. *Lab Chip* 2009;9:3504–10.
- [12] Kost GJ, Tran NK. Point-of-care testing and cardiac biomarkers: the standard of care and vision for chest pain centers. *Cardiol Clin* 2005;23:467–90.
- [13] Morrow DA, Cannon CP, Jesse RL, et al. National Academy of Clinical Biochemistry Laboratory Medicine Practice Guidelines: clinical characteristics and utilization of biochemical markers in acute coronary syndromes. *Clin Chem* 2007;53:552–74.
- [14] Apple FS, Parvin CA, Buechler KF, Christenson RH, Wu AHB, Jaffe AS. Validation of the 99th percentile cutoff independent of assay imprecision (CV) for cardiac troponin monitoring for ruling out myocardial infarction. *Clin Chem* 2005;51:2198–200.
- [15] Jonsson C, Aronsson M, Rundstrom G, et al. Silane-dextran chemistry on lateral flow polymer chips for immunoassays. *Lab Chip* 2008;8:1191–7.
- [16] Brooks DE, Devine DV, Harris PC, et al. RAMP (TM): A rapid, quantitative whole blood immunochromatographic platform for point-of-care testing. *Clin Chem* 1999;45:1676–8.
- [17] Muller-Bardorff M, Rauscher T, Kampmann H, et al. Quantitative bedside assay for cardiac troponin T: a complementary method to centralized laboratory testing. *Clin Chem* 1999;45:1002–8.
- [18] Apple FS, Murakami MM, Christenson RH, et al. Analytical performance of the i-STAT cardiac troponin I assay. *Clin Chim Acta* 2004;345:123–7.
- [19] Christenson RH, Azzazy HME. Cardiac point of care testing: a focused review of current National Academy of Clinical Biochemistry guidelines and measurement platforms. *Clin Biochem* 2009;42:150–7.
- [20] Yang Z, Zhou DM. Cardiac markers and their point-of-care testing for diagnosis of acute myocardial infarction. *Clin Biochem* 2006;39:771–80.
- [21] Friess U, Stark M. Cardiac markers: a clear cause for point-of-care testing. *Anal Bioanal Chem* 2009;393:1453–62.
- [22] Harrick NJ. Use of frustrated total internal reflection to measure film thickness and surface reliefs. *J Appl Phys* 1962;33:2774 &.
- [23] Prieve DC, Walz JY. Scattering of an evanescent surface-wave by a microscopic dielectric sphere. *Appl Opt* 1993;32:1629–41.
- [24] Tudos AJ, Besselink GAJ, Schasfoort RBM. Trends in miniaturized total analysis systems for point-of-care testing in clinical chemistry. *Lab Chip* 2001;1:83–95.